

# Defeating EpCAM<sup>+</sup> liver cancer stem cells by targeting chromatin remodeling enzyme CHD4 in human hepatocellular carcinoma

Kouki Nio, Taro Yamashita\*, Hikari Okada, Mitsumasa Kondo, Takehiro Hayashi, Yasumasa Hara, Yoshimoto Nomura, Sha Sha Zeng, Mariko Yoshida, Tomoyuki Hayashi, Hajime Sunagozaka, Naoki Oishi, Masao Honda, Shuichi Kaneko

Department of Gastroenterology, Kanazawa University Graduate School of Medical Science, Kanazawa, Ishikawa, Japan

**Background & Aims:** Hepatocellular carcinoma is composed of a subset of cells with enhanced tumorigenicity and chemoresistance that are called cancer stem (or stem-like) cells. We explored the role of chromodomain-helicase-DNA-binding protein 4, which is encoded by the *CHD4* gene and is known to epigenetically control gene regulation and DNA damage responses in EpCAM<sup>+</sup> liver cancer stem cells.

**Methods:** Gene and protein expression profiles were determined by microarray and immunohistochemistry in 245 and 144 hepatocellular carcinoma patients, respectively. The relationship between gene/protein expression and prognosis was examined. The functional role of CHD4 was evaluated in primary hepatocellular carcinoma cells and in cell lines *in vitro* and *in vivo*.

**Results:** CHD4 was abundantly expressed in EpCAM<sup>+</sup> hepatocellular carcinoma with expression of hepatic stem cell markers and poor prognosis in two independent cohorts. In cell lines, *CHD4* knockdown increased chemosensitivity and *CHD4* overexpression induced epirubicin chemoresistance. To inhibit the functions of CHD4 that are mediated through histone deacetylase and poly (ADP-ribose) polymerase, we evaluated the effect of the histone deacetylase inhibitor suberoylhydroxamic acid and the poly (ADP-ribose) polymerase inhibitor AG-014699. Treatment with either suberoylhydroxamic acid or AG-014699 reduced the number of EpCAM<sup>+</sup> liver cancer stem cells *in vitro*, and suberoylhydroxamic acid and AG-014699 in combination successfully inhibited tumor growth in a mouse xenograft model.

**Keywords:** Chromodomain-helicase-DNA-binding protein 4; Liver cancer stem cells; Histone deacetylase; Poly (ADP-ribose) polymerase; Chemoresistance.

Received 4 December 2014; received in revised form 3 June 2015; accepted 10 June 2015

\* Corresponding author. Address: Department of General Medicine/Gastroenterology, Kanazawa University Graduate School of Medical Science, 13-1 Takara-Machi, Kanazawa, Ishikawa 920-8641, Japan. Tel.: +81 76 265 2042; fax: +81 76 234 4281.

E-mail address: taroy@m-kanazawa.jp (T. Yamashita).

**Abbreviations:** AFP, alpha-fetoprotein; CHD, chromodomain-helicase-DNA-binding proteins; CSC, cancer stem cell; DSBs, double strand breaks; EpCAM, epithelial cell adhesion molecule; HCC, hepatocellular carcinoma; HDAC, histone deacetylase; HpSC, hepatic stem cell-like; NuRD, nucleosome remodeling and histone deacetylase; PARP, poly (ADP-ribose) polymerase; qRT-PCR, quantitative reverse transcription-polymerase chain reaction; SALL4, sal-like protein 4; SBHA, suberoylhydroxamic acid.

**Conclusions:** CHD4 plays a pivotal role in chemoresistance and the maintenance of stemness in liver cancer stem cells and is therefore a good target for the eradication of hepatocellular carcinoma.

© 2015 European Association for the Study of the Liver. Published by Elsevier B.V. All rights reserved.

## Introduction

Hepatocellular carcinoma (HCC) is one of the most common causes of cancer death worldwide [1,2]. This is partly due to a lack of effective chemotherapeutic options for patients with advanced-stage disease [3]. Various molecular profiling approaches have been used to identify potential therapeutic targets which are specifically activated in HCC [4–8]. Some studies have indicated the importance of evaluating “stemness” in HCC; it reflects the malignant nature of the tumor and closely correlates with a poor prognosis after surgery [9–12]. Recent evidence has also suggested that HCC may conform to the cancer stem cell (CSCs) hypothesis, which proposes that a subset of cells with stem cell features play a fundamental role in tumor maintenance and chemo/radiation resistance [13]. CSCs, also called tumor-initiating cells or cancer stem-like cells, possess stem cell features in their self-renewal and differentiation capacity, and contribute to the formation of heterogeneous tumor cell populations. In HCC, several stem cell markers, including CD133, CD90, CD13, epithelial cell adhesion molecule (EpCAM), and CD24, have been reported to enrich side populations of CSCs [13–15]. We recently reported that the stem cell markers EpCAM and alpha-fetoprotein (AFP) can be used to classify HCC subtypes with distinct gene expression profiles and patient prognoses [11]. In particular, the EpCAM<sup>+</sup> AFP<sup>+</sup> HCC subtype shares the gene expression features of cells from hepatic stem cell-like (HpSC)-HCC, and exhibits resistance to the chemotherapeutic reagent 5-fluorouracil [16,17]. However, the underlying molecular mechanisms which are responsible for the chemoresistance of EpCAM<sup>+</sup> CSCs remain to be identified.

Using gene expression profiling approaches, we recently identified the activation of transcription factor Sal-like protein 4 (SALL4) in EpCAM<sup>+</sup> CSCs from HpSC-HCC [18]. SALL4 is a



## Research Article

transcription factor which plays a fundamental role in the maintenance of embryonic stem cells, possibly through interaction with octamer-binding transcription factor 4, sex determining region Y-box 2, and Nanog [19–24]. It has been reported by three independent groups that SALL4 is a biomarker of HCCs with stem-like gene expression signatures and a poor prognosis [18,25,26]. SALL4 was recently found to directly interact with the epigenetic modulator nucleosome remodeling and histone deacetylase (NuRD) complex [27], thereby altering the histone modifications associated with stemness. Indeed, we have demonstrated that SALL4-positive HCCs have high histone deacetylase (HDAC) activity and are chemosensitive to HDAC inhibitors which reduce SALL4 expression [18].

The NuRD complex is a multi-unit chromatin remodeling complex consisting of chromodomain-helicase-DNA-binding proteins (CHDs), metastasis-associated proteins, and HDACs [28]. Interestingly, recent studies have indicated that CHD4, a DNA-binding protein which complexes with the NuRD complex, plays a role in the DNA damage/repair network and is recruited to DNA-damaged sites in a poly (ADP-ribose) polymerase (PARP)-dependent manner [29–32]. However, the role of CHD4 in the chemoresistance of EpCAM<sup>+</sup> CSCs remains to be elucidated. In this study, we investigated the role of CHD4, a NuRD complex protein which regulates HDAC activity and the DNA damage response, in the chemoresistance of liver CSCs. We further evaluated the efficacy of an HDAC inhibitor in combination with a PARP inhibitor in blocking CHD4 function in EpCAM<sup>+</sup> HCCs.

## Materials and methods

### Clinical HCC specimens

For microarray analyses, HCC tissues were obtained from 245 patients who had undergone radical resection from 2002 to 2003 at the Liver Cancer Institute (Fudan University, Shanghai, China). For immunohistochemical analyses, HCC tissues and adjacent non-cancerous liver tissues were obtained from 144 patients who had undergone a hepatectomy from 2002 to 2012 at Kanazawa University Hospital, Japan. The pathological diagnoses were performed as previously described [12]. Of these HCC specimens, 38 were obtained fresh and snap-frozen in liquid nitrogen for RNA analysis. An additional fresh HpSC-HCC sample was also obtained from surgical resection and used immediately to prepare a single-cell suspension. All tissue acquisition and experimental procedures were approved by the Ethics Committee and Institutional Review Board of each institute and conformed to the 1975 Declaration of Helsinki. All patients provided written informed consent.

### Cell culture and reagents

The human liver cancer cell lines HuH7, HuH1, Hep3B, HLE, HLF, and SK-Hep-1 were obtained from the Japanese Collection of Research Bioresources (Osaka, Japan) or the American Type Culture Collection (Manassas, VA) and were routinely cultured in Dulbecco's modified Eagle's medium (DMEM) supplemented with 10% fetal bovine serum (FBS). Primary HCC tissue samples were dissected and digested with 1 µg/ml type 4 collagenase solution (Sigma-Aldrich Japan K.K., Tokyo, Japan) at 37 °C for 15 min. Contaminating red blood cells were lysed with ammonium chloride solution (STEMCELL Technologies, Vancouver, Canada) on ice for 10 min. CD45<sup>+</sup> leukocytes and annexin V<sup>+</sup> apoptotic cells were removed from cell suspensions using an autoMACS-pro cell separator and magnet beads (MiltenyiBiotec K.K., Tokyo, Japan). The HDAC inhibitor suberoyhydroxamic acid (SBHA) and the PARP inhibitor AG-014699 were obtained from Cayman Chemical (Ann Arbor, MI) and Selleck Chemicals (Houston, TX), respectively. Inhibitor stock solutions were prepared in dimethyl sulfoxide and stored at –20 °C until use. The CHD4 expression plasmid pCMV6-AC-GFP-CHD4 (RG224232) was purchased from Origene Technologies, Inc. (Rockville, MD) and the pcDNA3.1 (V790-20) plasmid, which was used as an empty vector control, was purchased from Invitrogen (Carlsbad, CA). CHD4-specific and control siRNAs were purchased from

Dharmacon Research, Inc. (Lafayette, CO); the CHD4#1 and CHD4#2 siRNA sequences were “CCAGAAAGAGGAAUUGUCA” and “GGUUUAGUCUUAGAACA”, respectively. The siRNA constructs were transfected using Lipofectamine 2000 (Invitrogen) in accordance with the manufacturer's protocol.

### Quantitative reverse transcription-polymerase chain reaction (qRT-PCR)

Total RNA was extracted using TRIzol (Invitrogen) in accordance with the manufacturer's instructions. The expression of the selected genes was determined in triplicate using a 7900 Sequence Detection System (Applied Biosystems, Foster City, CA). Each sample was normalized relative to 18S ribosomal RNA expression. The following Applied Biosystems probes used were: CHD4, Hs00172349\_m1; EPCAM, Hs00158980\_m1; HDAC1, Hs02621185\_sl; AFP, Hs00173490\_m1; TERT, Hs00162669\_m1; BMI1, Hs00409825\_g1; POU5F1, Hs03005111\_g1; and 18S, Hs99999901\_s1.

### Western blotting

Whole cell lysates were prepared using radio-immunoprecipitation assay (RIPA) lysis buffer as previously described [33]. Anti-CHD4 monoclonal (Abcam, Cambridge, UK) and anti-β-actin monoclonal (Sigma-Aldrich Japan K.K.) antibodies were used for protein detection. Immune complexes were visualized using enhanced chemiluminescence detection reagents (Amersham Biosciences Corp., Piscataway, NJ) in accordance with the manufacturer's protocol.

### Immunohistochemistry and immunofluorescence

Immunohistochemistry was performed using an anti-CHD4 monoclonal primary antibody (Abcam) and Envision<sup>+</sup> kits (DAKO, Carpinteria, CA) in accordance with the manufacturer's instructions. CHD4 expression was evaluated and categorized as CHD4-high (score, 4–5) or CHD4-low (score, 0–3) based on the CHD4-staining score, which was the sum of the positivity score (0–5%, 0; 5–25%, 1; 25–50%, 2; and >50%, 3) and staining intensity score (weak, 0; moderate, 1; and strong, 2) for an area. Dual-color immunohistochemistry was performed using Vector red (Vector Laboratories Inc., Burlingame, CA) and the anti-EpCAM antibody VU-1D9 (Oncogene Research Products, San Diego, CA). For immunofluorescence, an Alexa Fluor<sup>®</sup> 488-conjugated anti-mouse immunoglobulin G secondary antibody (Molecular Probes, Carlsbad, CA) was used. Fluorescence microscopy was essentially performed as previously described [34]. Caspase-3 activation was determined by immunofluorescence using a cleaved caspase-3 (Asp175) antibody (Cell Signaling Technology Inc., Danvers, MA).

### Cell proliferation assays and fluorescence-activated cell sorting (FACS)

For cell proliferation assays,  $2 \times 10^3$  cells were seeded in 96-well plates and cell proliferation was evaluated in quadruplicate using the Cell Counting Kit-8 (DOJINDO LABORATORIES, Kumamoto, Japan). For flow cytometry and cell sorting, cells were trypsinized, washed, and resuspended in Hank's balanced salt solution (Lonza, Basel, Switzerland) supplemented with 1% HEPES and 2% FBS. Cells were incubated with the FITC-conjugated anti-EpCAM monoclonal antibody BER-EP4 (DAKO) on ice for 30 min prior to analysis using a FACSCalibur or FACSAriaII (BD Biosciences, San Jose, CA).

### Measurement of HDAC and PARP activity

HDAC and PARP activities were measured using the Epigenase HDAC Activity/Inhibition Direct Assay Kit (Epigentek Group Inc., Farmingdale, NY) and HT Universal Colorimetric PARP Assay Kit (Trevigen Inc., Gaithersburg, MD), respectively. Briefly, nuclear proteins were extracted using NE-PER Nuclear and Cytoplasmic Extraction Reagents (Thermo Fisher Scientific KK, Tokyo, Japan) and HDAC and PARP activity was measured in triplicate. Calculations were performed in accordance with the manufacturers' protocols.

### Animal studies

Cells ( $1 \times 10^5$  HuH7 or primary HCC cells, or  $3 \times 10^6$  HLF cells) were resuspended in 200 µl of a 1:1 DMEM: Matrigel (BD Biosciences) mixture and subcutaneously injected into 6-week-old non-obese diabetic/severe combined immunodeficiency mice (NOD/NCRCr1-Prkdc<sup>scid</sup>) which were purchased from Charles River Laboratories, Inc. (Wilmington, MA). For each cell type, 20 mice were inoculated.

The experimental protocol was approved by the Kanazawa University Animal Care and Use Committee and conformed to the Guide for the Care and Use of Laboratory Animals prepared by the National Academy of Sciences. The size and prevalence of subcutaneous tumors were recorded as previously described [34]. Once tumors had reached approximately 100 mm<sup>3</sup> (HuH7 and primary HCC cells) or 50 mm<sup>3</sup> (HLF cells), mice were randomized into treatment groups (n = 5 in each group). Mice were intraperitoneally injected with vehicle, 10 mg/kg AG-014699, 200 mg/kg SBHA, or AG-014699 and SBHA 3 times a week for 14 days.

#### Microarray studies and statistical analysis

Affymetrix U133A2.0 gene expression data were obtained from the National Center for Biotechnology Information Gene Expression Omnibus database (GEO accession number GSE14520), as previously described [35]. The BRB-ArrayTools software (version 4.3.2) was used for class comparison analyses. Hierarchical clustering analysis was performed using GENESIS software (version 1.7.6). To compare treatment groups in cell proliferation and qRT-PCR assays, Student's *t* tests and Chi-square tests were performed in GraphPad Prism software 6.0 (GraphPad Software, San Diego, CA). Kaplan–Meier survival analysis was also performed in GraphPad Prism software 6.0 (GraphPad Software). Univariate and multivariate Cox proportional hazards regression analysis was performed using SPSS software (SPSS Inc., Chicago, IL).

## Results

### High expression of CHD4 in EpCAM<sup>+</sup> liver CSCs

We evaluated the expression of CHD4 in EpCAM<sup>+</sup> and EpCAM<sup>-</sup> cells using a HuH7 single-cell suspension. We found that CHD4 was up-regulated in EpCAM<sup>+</sup> cells compared with EpCAM<sup>-</sup> cells (Fig. 1A). Using immunofluorescence imaging, a strong nuclear accumulation of CHD4 was identified in the isolated EpCAM<sup>+</sup> cells (Fig. 1B and Supplementary Fig. 1A). Similar results were also observed in purified EpCAM<sup>+</sup> and EpCAM<sup>-</sup> cells obtained from a primary HCC specimen (Supplementary Fig. 1B). To explore the relationship between CHD4 and EpCAM expression in HCC and confirm the nuclear accumulation of CHD4 in HCC tissues, we analyzed 144 surgically resected HCC specimens (cohort 1) using immunohistochemistry. Interestingly, the abundance of CHD4<sup>+</sup> cells varied dramatically in each HCC specimen (Fig. 1C). We evaluated the expression of CHD4 in terms of staining intensity and the number of positively stained cells, and categorized HCC tissues as CHD4-high or CHD4-low according to the criteria described in the Materials and methods section. Using these criteria, 50 of the 144 HCCs (34.7%) were classified as CHD4-high HCCs. An analysis of the clinicopathological characteristics of CHD4-high and CHD4-low HCCs suggested that the CHD4-high HCCs were significantly associated with a poorly differentiated morphology, large tumor size, and EpCAM and CK19 expression (Table 1). The co-expression of CHD4 and EpCAM in HCC tissues was confirmed by dual-color immunohistochemical analysis (Supplementary Fig. 1C). Kaplan–Meier survival analysis indicated that, following surgery, CHD4-high HCCs are statistically significantly associated with a poorer survival compared to CHD4-low HCCs ( $p = 0.036$ ; Fig. 1D). Given that the expression of CHD4 and EpCAM did not completely overlap in the HCC samples (Table 1), we performed a separate evaluation of the effect of CHD4 expression on the survival of EpCAM<sup>+</sup> and EpCAM<sup>-</sup> HCC patients (Supplementary Fig. 1D). As expected, CHD4-low EpCAM<sup>-</sup> HCCs showed better survival than other subclasses. CHD4-high EpCAM<sup>+</sup> HCCs showed a worse prognosis than CHD4-low EpCAM<sup>+</sup> HCCs, but this difference was not statistically significant. Interestingly, CHD4-high EpCAM<sup>-</sup> HCCs showed a

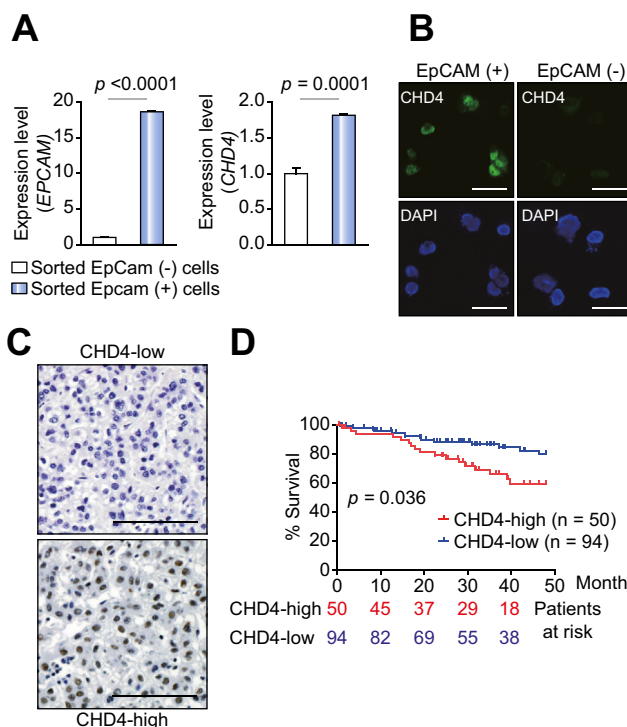


**Fig. 1. High expression of chromodomain-helicase-DNA-binding protein 4 (CHD4) in epithelial cell adhesion molecule (EpCAM)<sup>+</sup> cancer stem cells (CSCs).** (A) Quantitative reverse transcription-polymerase chain reaction (qRT-PCR) analysis of *CHD4* and *EpCAM* in HuH7 cells. EpCAM<sup>+</sup> and EpCAM<sup>-</sup> HuH7 cells were isolated by FACS sorting; (B) Immunofluorescence analysis of CHD4 in EpCAM<sup>+</sup> and EpCAM<sup>-</sup> HuH7 cells (scale bar, 50 μm). (C) Immunohistochemical analysis of CHD4 in surgically resected hepatocellular carcinomas (HCCs). Representative photomicrographs of CHD4-high (right panel) and CHD4-low (left panel) HCC tissues are shown (scale bar, 100 μm). (D) Kaplan–Meier survival curves for 144 patients who underwent surgery. CHD4-high HCCs (n = 50) showed a poor prognosis compared with CHD4-low HCCs (n = 94).

worse prognosis than CHD4-low EpCAM<sup>-</sup> HCCs, and this difference was statistically significant ( $p = 0.03$ ). These analyses suggest that CHD4 expression impacts HCC survival, even in EpCAM<sup>-</sup> HCCs. We therefore evaluated the prognostic value of CHD4 expression on survival, relative to other clinicopathological parameters, in cohort 1 using univariate and multivariate Cox regression analysis (Supplementary Tables 1 and 2). Although high CHD4 expression, tumor size, portal vein invasion, Barcelona Clinic Liver Cancer (BCLC) stage, histology, and serum AFP were all associated with a poor survival in univariate analysis, multivariate analysis indicated that only the BCLC stage was an independent risk factor for poor survival in HCC. This suggests that CHD4 expression might be a confounding factor in HCC and is not sufficient, on its own, for evaluating the survival outcome of HCC.

### Transcriptomic characteristics of CHD4-high HCCs

To evaluate the molecular profiles of CHD4-high HCCs, we analyzed an Affymetrix gene expression dataset of 245 primary HCC tissues (cohort 2). We defined top-tertile of all HCCs (83 of 245) as CHD4-high when ordered according to the *CHD4* signal intensities. The difference between *CHD4* gene expression in



## Research Article

Table 1. Clinicopathological characteristics of CHD4-high and CHD4-low HCCs.

Parameter	CHD4-high (n = 50)	CHD4-low (n = 94)	p value*
Mean age, y (SD)	62.8 (9.5)	63.6 (9.9)	0.63
Sex: male/female	37/13	67/27	0.85
Mean AFP level, ng/ml (SD)	9931 (55,278)	639.5 (2220)	0.11
Histologic grade**: I-II/III-III/III-IV	5/30/15	16/71/7	0.0014
Mean tumor size, mm (SD)	41.8 (28.2)	31.6 (19.0)	0.048
Macroscopic portal vein invasion: yes/no	14/36	18/76	0.29
BCLC stage: 0/A/B/C	4/23/7/16	20/47/7/20	0.09
Virus status: B/C/B + C/NBNC	17/22/2/9	21/57/1/15	0.19
EpCAM: positive/negative	26/24	30/64	0.02
CK19: positive/negative	15/35	9/85	0.004

CHD4, chromodomain-helicase-DNA-binding protein 4; HCC, hepatocellular carcinoma; SD, standard deviation; AFP, alpha-fetoprotein; BCLC, Barcelona Clinic Liver Cancer; B, hepatitis B surface (HBs) antigen positive; C, hepatitis C virus (HCV) antibody positive; B + C, HBs antigen positive and HCV antibody positive; NBNC, HBs antigen negative and HCV antibody negative; EpCAM, epithelial cell adhesion molecule.

\*Mann-Whitney U test, Chi-square test, or Fisher's exact test.

\*\*Edmondson-Steiner grading.

CHD4-high and CHD4-low HCCs was 1.62-fold (Supplementary Fig. 2A). Similarly, the difference between CHD4 gene expression in CHD4-high and CHD4-low HCCs defined by immunohistochemistry was 1.86-fold in cohort 1, evaluated by qRT-PCR (Supplementary Fig. 2B). This demonstrates a concordance between the gene and protein expression criteria for CHD4-high and CHD4-low HCCs in the two cohorts. The clinicopathological characteristics of CHD4-high and CHD4-low HCCs in cohort 2 (Supplementary Table 3) indicate that serum AFP was significantly higher in CHD4-high HCCs than in CHD4-low HCCs ( $p = 0.015$ ). We performed a class comparison analysis with  $t$  tests ( $p < 0.001$ ) and permutation tests ( $p < 0.001$ , computed based on 10,000 random permutations) of the class labels (CHD4-high and CHD4-low) using BRB-ArrayTools (version 4.3.2) to evaluate the genes differentially expressed between the classes and to control the number and proportion of false discoveries of genes identified. We identified a total of 724 genes that were differentially expressed with  $\geq 1.2$ -fold difference between the two HCC subclasses (the complete gene list with parametric  $p$  values, false discovery rates, and permutation  $p$  values of identified genes is available in Supplementary Table 4). Of these genes, 329 were up-regulated and 395 were down-regulated in CHD4-high HCCs (Fig. 2A). Interestingly, stemness-related genes, such as *SOX9* and *KRT19*, and Wnt/TGF- $\beta$  pathway related genes, including *TGFB1* and *TCF4*, were up-regulated in CHD4-high HCCs. Genes associated with the epigenetic control of transcription, such as *JARID1A* and *ARID3A*, were also up-regulated in CHD4-high HCCs. Furthermore, the genes related to mature hepatocyte function (e.g., those involved in serum production and xenobiotic metabolism), such as *F8*, *F13B*, *C6*, *C8B*, *CYP4F2*, and *CYP2C9*, were down-regulated in CHD4-high HCCs. We proceeded to evaluate the expression of CHD4 in EpCAM<sup>+</sup> AFP<sup>+</sup> HCCs (HpSC-HCCs) and EpCAM<sup>-</sup> AFP<sup>-</sup> HCCs (Mature hepatocyte-like HCCs; MH-HCCs). These are HCC subclasses which we previously proposed as being associated with the stem/maturation status of HCCs [11]. As expected, CHD4 expression was significantly higher in HpSC-HCCs compared with MH-HCCs ( $p = 0.0026$ ; Supplementary Fig. 3). Consistent with this, pathway analysis indicated that the Wnt/TGF- $\beta$  pathway, Sin3/NuRD transcriptional regulation, and the epigenetic regulation of gene expression were all activated in CHD4-high HCCs (Fig. 2B). In contrast, in CHD4-low

HCCs, pathways associated with mature hepatocyte function, such as PPAR-regulated lipid metabolism, and cholesterol and sphingolipid transport, were activated (Fig. 2C). The statistically significant poor prognosis of CHD4-high HCCs was independently validated in the cohort 2 microarray data ( $p = 0.029$ ; Fig. 2D). This suggests that CHD4-high HCCs represent a HCC subtype with a stem cell-like gene expression signature and a poor prognosis.

#### CHD4 confers chemoresistance in EpCAM<sup>+</sup> HCCs

To evaluate the functional role of CHD4 in HCC, we transiently knocked down CHD4 gene expression in EpCAM<sup>+</sup> HuH7 cells using two CHD4-specific siRNAs (CHD4#1 and CHD4#2). CHD4 expression decreased in HuH7 cells transfected with CHD4 siRNAs compared with those transfected with a control siRNA (Fig. 3A). Interestingly, CHD4 knockdown enhanced chemosensitivity to epirubicin in HuH7 cells (Fig. 3B). Similar results were also obtained using HuH1 and Hep3B cells (Supplementary Fig. 4A and 4B). We further evaluated the effect of CHD4 overexpression in HuH1 cells. We transfected HuH1 cells with either an empty vector control (pcDNA 3.1) or a CHD4-encoding plasmid (pCMV6-CHD4) and confirmed the up-regulation of CHD4 transcript and protein (Fig. 3C). CHD4 overexpression clearly enhanced epirubicin chemoresistance in HuH1 cells (Fig. 3D). Again, similar results were obtained using HuH7 and Hep3B cells (Supplementary Fig. 4C and 4D). Taken together, these data suggest that CHD4 plays a pivotal role in the chemoresistance of EpCAM<sup>+</sup> HCC.

#### Overcoming EpCAM<sup>+</sup> HCC by targeting CHD4 through HDAC/PARP inhibition

The above data demonstrate that the activation of CHD4 may play a fundamental role in the chemoresistance of EpCAM<sup>+</sup> CSCs to cytotoxic reagents, suggesting that CHD4 suppression may be useful for the eradication of EpCAM<sup>+</sup> CSCs. We recently demonstrated that HDACs are activated in EpCAM<sup>+</sup> HCCs, and that HDAC inhibitors successfully inhibit the growth of EpCAM<sup>+</sup> HCC cell lines [18]. We evaluated the expression of HDAC1 in 38 surgically resected snap-frozen specimens using qRT-PCR. The analysis indicated a concordant up-regulation of HDAC1 in CHD4-high

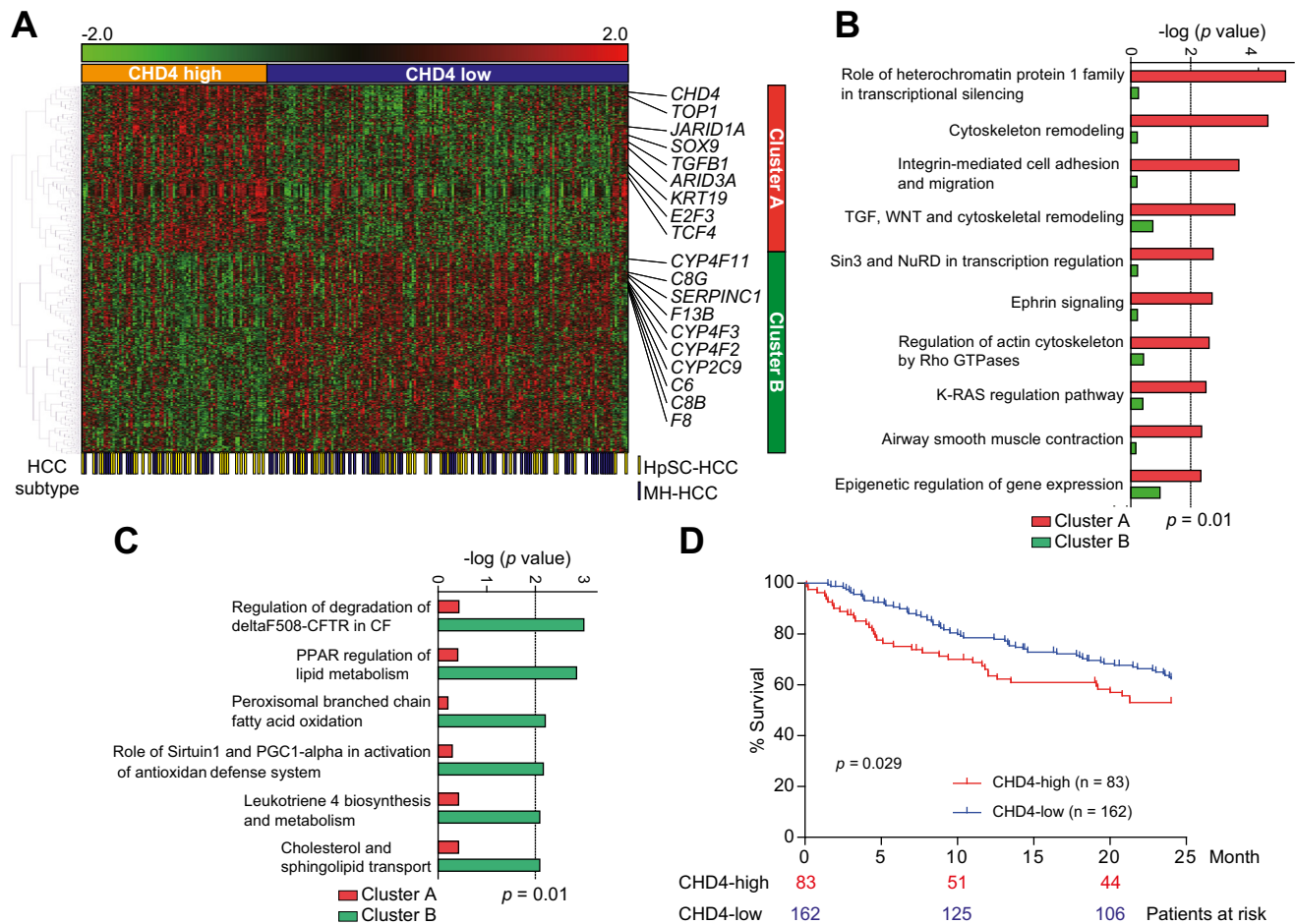


**Fig. 2. Transcriptome analysis of CHD4-high and CHD4-low HCCs.** (A) Hierarchical cluster analysis of 726 genes with  $\geq 1.2$ -fold difference in expression between CHD4-high and CHD4-low HCCs. In CHD4-high HCCs, 329 genes (Cluster A) and 395 genes (Cluster B) were up-regulated and down-regulated, respectively. Each cell in the matrix represents the expression of a gene in an individual sample. Red and green cells depict high and low expression levels, respectively, as indicated by the scale bar (fold change in expression). EpCAM<sup>+</sup> AFP<sup>+</sup> HCCs (Hepatic stem cell-like HCCs; HpSC-HCCs) and EpCAM<sup>-</sup> AFP<sup>-</sup> HCCs (Mature hepatocyte-like HCCs; MH-HCCs) are depicted as yellow and blue boxes, respectively. Representative genes associated with hepatic stem/maturation status are listed. (B & C) Pathway analysis of CHD4-co-regulated genes. The signaling pathways which were activated in CHD4-high (cluster A) and CHD4-low (cluster B). HCCs with statistical significance ( $p < 0.01$ ) are shown. (D) Kaplan-Meier survival curves for 235 patients who underwent surgery. CHD4-high HCCs ( $n = 83$ ) showed a poorer prognosis than CHD4-low HCCs ( $n = 162$ ).

HCCs ( $n = 13$ ) compared with CHD4-low ( $n = 25$ ) HCCs ( $p = 0.039$ ; [Supplementary Fig. 5](#)). Recent studies have demonstrated the role of CHD4, in collaboration with PARP, in repairing double strand breaks (DSBs) in cancer cells [31]. We have confirmed that CHD4 protein rapidly co-localizes with phosphorylated histone H2AX immediately after epirubicin treatment ([Supplementary Fig. 6](#)). Taken together, these data suggest that CHD4, with HDAC and PARP, may maintain EpCAM<sup>+</sup> liver CSCs by forming part of the NuRD complex and regulating the cellular histone status and DNA damage response. Therefore, we hypothesized that the combination of an HDAC inhibitor with a PARP inhibitor may be efficacious in suppressing CHD4 function in EpCAM<sup>+</sup> liver CSCs.

We proceeded to assess HDAC and PARP activity in HuH7 cells treated with the HDAC inhibitor SBHA and the PARP inhibitor AG-014699; SBHA and AG-014699 suppressed HDAC and PARP activities in HuH7 cells in a specific manner ([Fig. 4A](#)). We then evaluated the effect of SBHA and AG-014699 on EpCAM<sup>+</sup> CSCs

using fluorescence-activated cell sorting. SBHA and AG-014699 treatment reduced the number of EpCAM<sup>+</sup> CSCs compared with control treatment ([Fig. 4B](#)). Consistent with this, the treatment of HuH7 cells with SBHA or AG-014699 suppressed the expression of stemness-related genes such as *EpCAM*, *AFP*, *TERT*, *BMI1*, and *POU5F1*, in addition to *CHD4* ([Fig. 4C](#)). No additive reduction in the population of EpCAM<sup>+</sup> cells was observed with combined SBHA and AG-014699 treatment ([Supplementary Fig. 7](#)). We also evaluated the effect of AG-014699 on the early recruitment of CHD4 to the site of DSBs. In HuH7 cells treated with epirubicin for 30 min, AG-014699 suppressed the nuclear co-localization of CHD4 with phosphorylated histone H2AX ([Supplementary Fig. 8](#)).

To evaluate the chemosensitivity of CHD4-high and CHD4-low HCCs to SBHA and AG-014699, we evaluated the expression of CHD4 in EpCAM<sup>+</sup> AFP<sup>+</sup> cell lines (Hep3B, HuH7, and HuH1) and EpCAM<sup>-</sup> AFP<sup>-</sup> HCC cell lines (SK-Hep-1, HLE, and HLF). Consistent with the primary HCC data, EpCAM<sup>+</sup> AFP<sup>+</sup> HCC cell lines

## Research Article

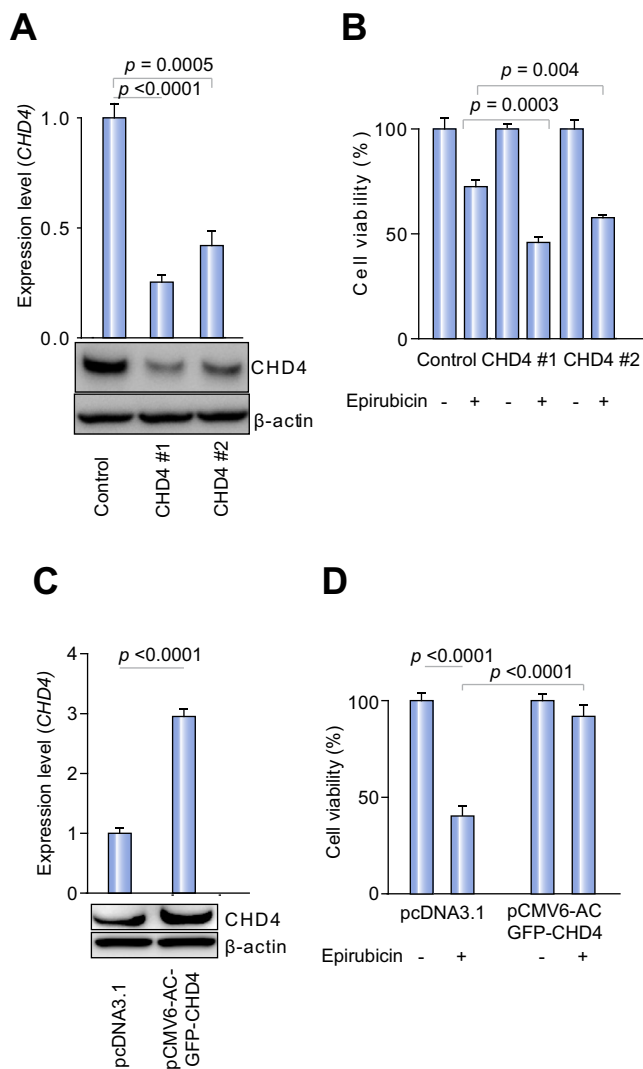


**Fig. 3. Regulation of chemoresistance by CHD4.** (A) Upper panel: qRT-PCR analysis of HuH7 cells transfected with CHD4-specific siRNAs (CHD4#1 and CHD4#2) or scramble control siRNA (Control). Lower panel: Western blot analysis of HuH7 cells transfected with CHD4-specific siRNAs or scramble control siRNA. (B) Chemosensitization of HuH7 cells by CHD4 knockdown. HuH7 cells were transfected with CHD4-specific or control siRNAs, treated with 0.2 μg/ml epirubicin, and cellular viability was analyzed. (C) Upper panel: qRT-PCR analysis of HuH1 cells transfected with pcDNA3.1 control plasmid or pCMV6-AC-GFP-CHD4 plasmid. Lower panel: Western blot analysis of HuH1 cells transfected with pcDNA3.1 control plasmid or pCMV6-AC-GFP-CHD4 plasmid. (D) The chemoresistance of HuH1 cells was enhanced by CHD4 overexpression. HuH1 cells were transfected with pcDNA3.1 control plasmid or pCMV6-AC-GFP-CHD4 plasmid, treated with 0.2 μg/ml epirubicin, and cell viability was analyzed.

expressed high levels of CHD4 protein compared with EpCAM<sup>-</sup>AFP<sup>-</sup> HCC cell lines (Fig. 5A). Treatment of HuH1, HuH7, HLE, and HLF cells with 10 μM SBHA or AG-014699 indicated that both reagents inhibited the proliferation of HuH1 and HuH7 cells but had relatively little effect on the proliferation of HLE and HLF cells (Fig. 5B and 5C). Furthermore, the combination of SBHA and AG-014699 produced an additive effect on HuH1 and HuH7 cellular proliferation compared with either treatment alone (Fig. 5D and 5E). The treatment of HuH7 cells

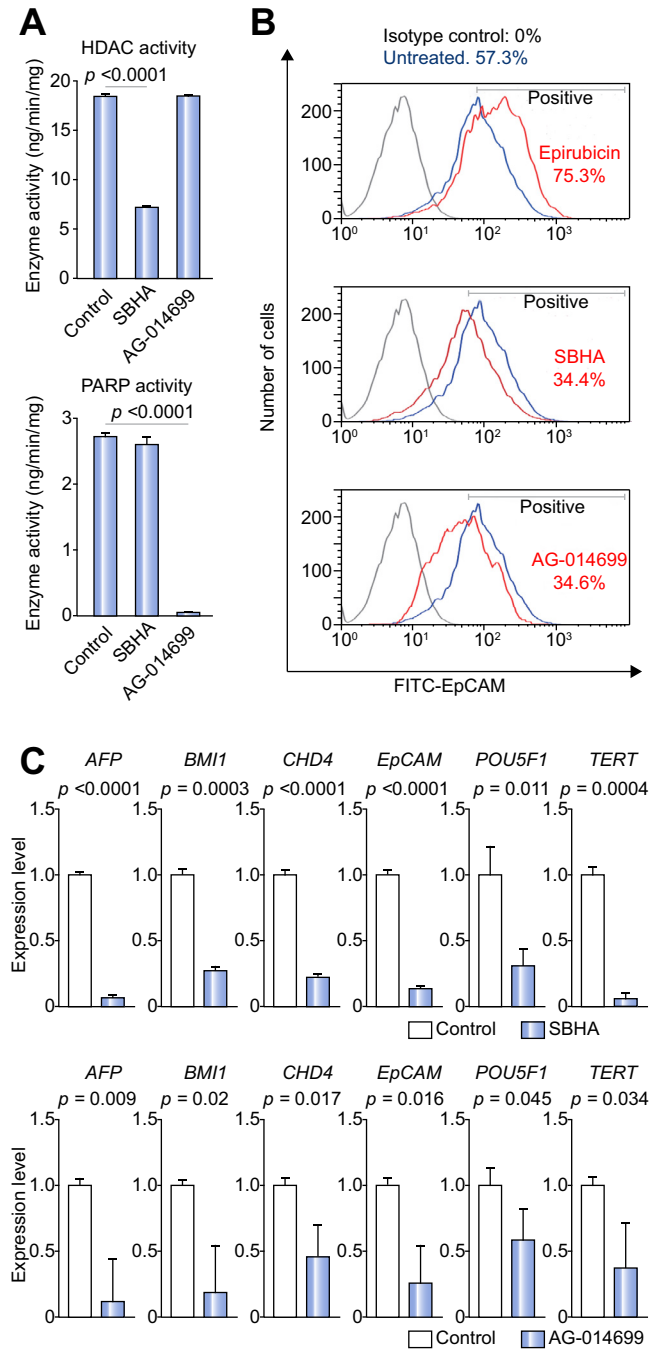


**Fig. 4. Effect of the histone deacetylase (HDAC) inhibitor suberoylohydroxamic acid (SBHA) and the poly (ADP-ribose) polymerase (PARP) inhibitor AG-014699 on HuH7 cells.** (A) HDAC (upper panel) and PARP (lower panel) activity in protein extracts from HuH7 cells treated with 20 μM SBHA or 15 μM AG-014699. (B) FACS of HuH7 cells. Untreated HuH7 cells or HuH7 cells treated with 0.2 μg/ml epirubicin, 20 μM SBHA, or 15 μM AG-014699 for 7 days were stained with a fluorescein isothiocyanate-EpCAM antibody or an isotype control antibody. (C) Upper panels: qRT-PCR analysis of HuH7 cells treated with dimethyl sulfoxide (control) or 20 μM SBHA for 7 days. Lower panels: qRT-PCR analysis of HuH7 cells treated with control dimethyl sulfoxide (control) or 15 μM AG-014699 for 7 days.

with SBHA or AG-014699 also increased caspase-3 activation (Supplementary Fig. 9A and 9B), indicating that the observed

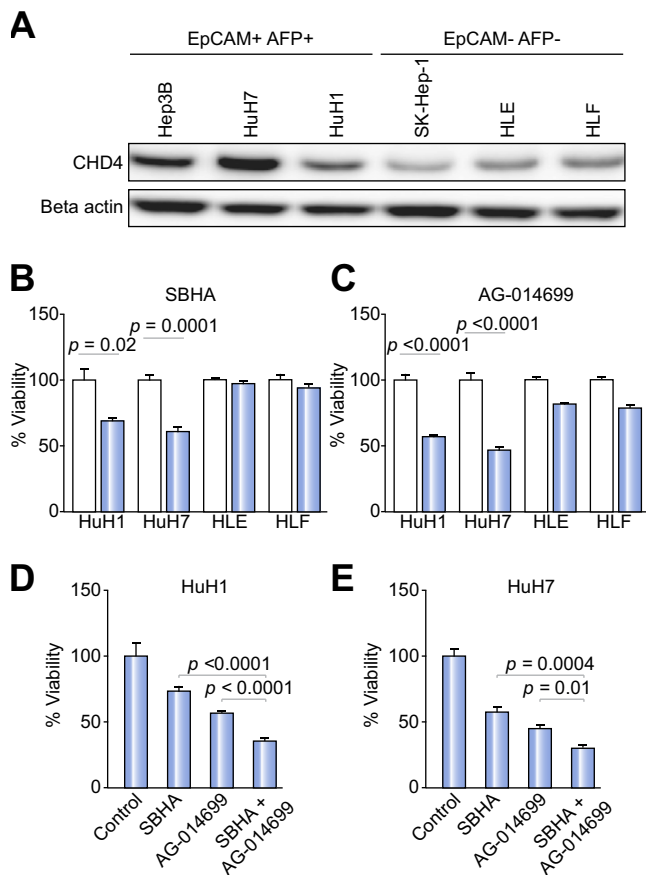


**Fig. 5. Effect of the HDAC inhibitor SBHA and the PARP inhibitor AG-014699 on CHD4-high and CHD4-low HCC cell lines.** (A) CHD4 expression in EpCAM<sup>+</sup> alpha-fetoprotein (AFP)<sup>+</sup> and EpCAM<sup>-</sup> AFP<sup>-</sup> HCC cell lines was evaluated by Western blotting. (B) The effect of 10  $\mu$ M SBHA on HuH1, HuH7, HLE, and HLF cell growth. (C) The effect of 10  $\mu$ M AG-014699 on HuH1, HuH7, HLE, and HLF cell growth. (D & E) The effect of 20  $\mu$ M SBHA and 15  $\mu$ M AG-014699 on the growth of HuH1 (D) and HuH7 (E) cells.

inhibition of cellular proliferation with SBHA or AG-014699 treatment is likely due to the stimulation of apoptosis signaling in these cells.

Finally, we evaluated the effect of SBHA and AG-014699 combination therapy on HuH7 and primary EpCAM<sup>+</sup> HCC cells *in vivo* using a subcutaneous mouse xenograft model. SBHA or AG-014699 treatment alone had limited effects on tumor growth compared with the control (SBHA,  $p = 0.3$ ; AG-014699,  $p = 0.73$ ). However, the combination of SBHA and AG-014699 successfully inhibited HCC tumor growth compared with control ( $p = 0.04$ ) (Fig. 6A). The number of CHD4-positive cells in tumors was also decreased with the combination therapy compared with control treatment (Fig. 6B and 6C). Similar results were also obtained in primary EpCAM<sup>+</sup> HCC cells (Supplementary Fig. 10A and 10B). Interestingly, the inhibitory effects of SBHA and AG-014699 on tumorigenicity were not observed in EpCAM<sup>-</sup> HLF cell NOD/SCID mice tumor xenografts (Supplementary Fig. 11).

Taken together, our data demonstrate, for the first time, the pivotal role of CHD4 in the maintenance and chemoresistance of EpCAM<sup>+</sup> CSCs. CHD4 is activated in EpCAM<sup>+</sup> CSCs and is

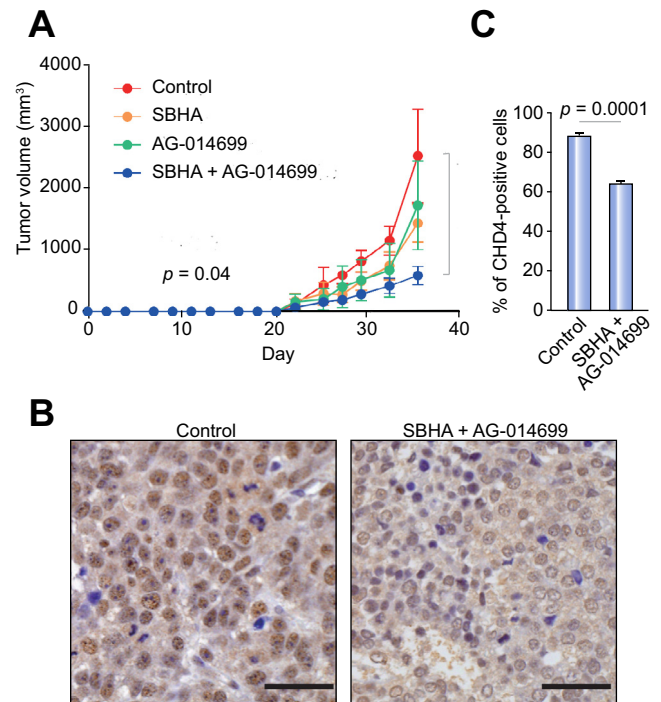


**Fig. 6. Suppression of HCC growth by SBHA and AG-014699 *in vivo*.** (A) The effect of the HDAC inhibitor SBHA and the PARP inhibitor AG-014699 on the growth of HuH7 cells. (B) Representative images of CHD4 staining in HuH7 tumor xenografts in control and SBHA + AG-014699-treated mice (scale bar, 100  $\mu$ m). (C) The number of nuclear CHD4-positive cells in HuH7 tumor xenografts in control and SBHA + AG-014699-treated mice.

recruited to sites of DNA damage when DSBs occur in the nucleus. The inhibition of HDAC and PARP, using molecularly targeted reagents, dramatically suppresses the number of EpCAM<sup>+</sup> CSCs, reduces CHD4 expression, and successfully inhibits EpCAM<sup>+</sup> HCC growth.

## Discussion

Stemness traits in cancer cells are currently of great interest because they may explain the malignant nature of tumors, and therefore the clinical outcome of patients [13]. Recently, we proposed a HCC classification system based on the stem/maturation status of tumors based on EpCAM and AFP expression [11]. These HCC subtypes showed distinct gene expression patterns with features resembling particular stages of liver lineages. Among them, HpSC-HCC (EpCAM<sup>+</sup> AFP<sup>+</sup>) was characterized by a highly invasive nature, particularly to the vessels, chemoresistance to cytotoxic reagents, and a poor patient prognosis after radical resection. This highlights the need to develop a novel therapeutic approach for this HCC subtype [17].

In the present study, we showed that CHD4, a member of the NuRD complex together with HDAC, regulates chromatin remodeling and HDAC activities, and is activated in EpCAM<sup>+</sup> CSCs. Consistent with this, recent studies have indicated that epigenetic dysregulation contributes to the maintenance of a malignant phenotype in HCC [36,37]. The cellular abundance of CHD4 may relate to the malignant nature of the tumor, and might therefore



## Research Article

be used to stratify HCC patient prognosis after surgery. CHD4 is a catalytic subunit of the NuRD transcriptional repressor complex, but recent studies have also demonstrated that CHD4 is rapidly recruited to sites of DNA damage in a PARP-dependent manner [29–32]. Therefore, the activation of CHD4 in CSCs may play a dual role in maintaining stemness characteristics and enhancing chemoresistance to DNA damage reagents.

High levels of CHD4 expression may confer resistance to chemotherapeutic reagents which induce DSBs. Recent studies have shown the importance of CHD4 in response to ionizing radiation and PARP inhibitors [29–32,38]. In this study, we demonstrated that CHD4 plays a role in the resistance to epirubicin, which induces DSBs in cancer cells. Epirubicin is widely used to treat HCC by transcatheter hepatic arterial chemoembolization, although the utility of this treatment is considered to be limited due to drug/hypoxia resistance in HCC cells. We have shown that CHD4 suppression enhances epirubicin chemosensitivity in EpCAM<sup>+</sup> HCC cells. Given that the recruitment of PARP and CHD4 to sites of DNA damage is believed to set up a transient repressive chromatin structure which facilitates DNA damage repair, our data suggest that PARP inhibitors could block NuRD complex recruitment and facilitate DNA damage in EpCAM<sup>+</sup> liver CSCs.

The combination of SBHA and AG-014699 was most effective at treating HpSC-HCC. SBHA treatment suppressed the HpSC-HCC stemness traits with a reduction in the number of EpCAM<sup>+</sup> cells, and AG-014699 treatment further suppresses the recruitment of CHD4 during the DNA damage response. A recent study has shown that a combination therapy of HDAC and PARP inhibitors is effective for treating HCC [39], and our findings provide mechanistic insights into how HDAC and PARP inhibitors work to eradicate EpCAM<sup>+</sup> liver CSCs. The safety, tolerability, and efficacy of this combination therapy for HCC patients warrants further investigation in a clinical setting.

### Financial support

This study was supported by Grant-in-Aid from the Ministry of Education, Culture, Sports, Science and Technology (No. 23590967 and 26460994), a grant from the Ministry of Health, Labour and Welfare, a grant from the National Cancer Center Research and Development Fund (23-B-5), and a grant from the Project for Development of Innovative Research on Cancer Therapeutics.

### Conflicts of interest

The authors who have taken part in this study declared that they do not have anything to disclose regarding funding or conflict of interest with respect to this manuscript.

### Authors' contributions

Kouki Nio: acquisition and analysis of data, preparation of manuscript; Taro Yamashita: study concept and design, acquisition, analysis, and interpretation of data, preparation of manuscript; Hikari Okada, Mitsumasa Kondo, Takehiro Hayashi, Yasumasa

Hara, Yoshimoto Nomura, Sha Sha Zeng, Mariko Yoshida, Tomoyuki Hayashi, Hajime Sunagozaka, and Naoki Oishi: acquisition of data; Masao Honda and Shuichi Kaneko: study design and supervision.

### Acknowledgements

We thank Ms. Masayo Baba, Nami Nishiyama, and Mikiko Nakamura for technical assistance. This study was supported by Grant-in-Aid from the Ministry of Education, Culture, Sports, Science, and Technology (No. 23590967 and 26460994), a grant from the Ministry of Health, Labour and Welfare, a grant from the National Cancer Center Research and Development Fund (23-B-5), and a grant from the Project for Development of Innovative Research on Cancer Therapeutics.

### Supplementary data

Supplementary data associated with this article can be found, in the online version, at <http://dx.doi.org/10.1016/j.jhep.2015.06.009>.

### References

- [1] Jemal A, Bray F, Center MM, Ferlay J, Ward E, Forman D. Global cancer statistics. *CA Cancer J Clin* 2011;61:69–90.
- [2] Bruix J, Gores GJ, Mazzaferro V. Hepatocellular carcinoma: clinical frontiers and perspectives. *Gut* 2014;63:844–855.
- [3] de Lope CR, Tremosini S, Forner A, Reig M, Bruix J. Management of HCC. *J Hepatol* 2012;56:S75–S87.
- [4] Hoshida Y, Nijman SM, Kobayashi M, Chan JA, Brunet JP, Chiang DY, et al. Integrative transcriptome analysis reveals common molecular subclasses of human hepatocellular carcinoma. *Cancer Res* 2009;69:7385–7392.
- [5] Ji J, Shi J, Budhu A, Yu Z, Forgues M, Roessler S, et al. MicroRNA expression, survival, and response to interferon in liver cancer. *New Engl J Med* 2009;361:1437–1447.
- [6] Shibata T, Aburatani H. Exploration of liver cancer genomes. *Nat Rev Gastroenterol Hepatol* 2014;11:340–349.
- [7] Guichard C, Amaddeo G, Imbeaud S, Ladeiro Y, Pelletier L, Maad IB, et al. Integrated analysis of somatic mutations and focal copy-number changes identifies key genes and pathways in hepatocellular carcinoma. *Nat Genet* 2012;44:694–698.
- [8] Nault JC, Mallet M, Pilati C, Calderaro J, Bioulac-Sage P, Laurent C, et al. High frequency of telomerase reverse-transcriptase promoter somatic mutations in hepatocellular carcinoma and preneoplastic lesions. *Nat Commun* 2013;4:2218.
- [9] Kim H, Yoo JE, Cho JY, Oh BK, Yoon YS, Han HS, et al. Telomere length, TERT and shelterin complex proteins in hepatocellular carcinomas expressing “stemness”-related markers. *J Hepatol* 2013;59:746–752.
- [10] Lee JS, Heo J, Libbrecht L, Chu IS, Kaposi-Novak P, Calvisi DF, et al. A novel prognostic subtype of human hepatocellular carcinoma derived from hepatic progenitor cells. *Nat Med* 2006;12:410–416.
- [11] Yamashita T, Forgues M, Wang W, Kim JW, Ye Q, Jia H, et al. EpCAM and alpha-fetoprotein expression defines novel prognostic subtypes of hepatocellular carcinoma. *Cancer Res* 2008;68:1451–1461.
- [12] Yamashita T, Kitao A, Matsui O, Hayashi T, Nio K, Kondo M, et al. Gd-EOB-DTPA-enhanced magnetic resonance imaging and alpha-fetoprotein predict prognosis of early-stage hepatocellular carcinoma. *Hepatology* 2014;60:1674–1685.
- [13] Yamashita T, Wang XW. Cancer stem cells in the development of liver cancer. *J Clin Investig* 2013;123:1911–1918.
- [14] Yamashita T, Honda M, Nakamoto Y, Baba M, Nio K, Hara Y, et al. Discrete nature of EpCAM(+) and CD90(+) cancer stem cells in human hepatocellular carcinoma. *Hepatology* 2013;57:1484–1497.
- [15] Lee TK, Castilho A, Cheung VC, Tang KH, Ma S, Ng IO. CD24(+) liver tumor-initiating cells drive self-renewal and tumor initiation through STAT3-mediated NANOG regulation. *Cell Stem Cell* 2011;9:50–63.



- [16] Yamashita T, Budhu A, Forgues M, Wang XW. Activation of hepatic stem cell marker EpCAM by Wnt-beta-catenin signaling in hepatocellular carcinoma. *Cancer Res* 2007;67:10831–10839.
- [17] Yamashita T, Ji J, Budhu A, Forgues M, Yang W, Wang HY, et al. EpCAM-positive hepatocellular carcinoma cells are tumor-initiating cells with stem/progenitor cell features. *Gastroenterology* 2009;136:1012–1024.
- [18] Zeng SS, Yamashita T, Kondo M, Nio K, Hayashi T, Hara Y, et al. The transcription factor SALL4 regulates stemness of EpCAM-positive hepatocellular carcinoma. *J Hepatol* 2014;60:127–134.
- [19] Rao S, Zhen S, Roumiantsev S, McDonald LT, Yuan GC, Orkin SH. Differential roles of Sall4 isoforms in embryonic stem cell pluripotency. *Mol Cell Biol* 2010;30:5364–5380.
- [20] Tanimura N, Saito M, Ebisuya M, Nishida E, Ishikawa F. Stemness-related Factor Sall4 Interacts with Transcription Factors Oct-3/4 and Sox2 and Occupies Oct-Sox Elements in Mouse Embryonic Stem Cells. *J Biol Chem* 2013;288:5027–5038.
- [21] Wu Q, Chen X, Zhang J, Loh YH, Low TY, Zhang W, et al. Sall4 interacts with Nanog and co-occupies Nanog genomic sites in embryonic stem cells. *J Biol Chem* 2006;281:24090–24094.
- [22] Yang J, Chai L, Fowles TC, Alipio Z, Xu D, Fink LM, et al. Genome-wide analysis reveals Sall4 to be a major regulator of pluripotency in murine-embryonic stem cells. *Proc Natl Acad Sci USA* 2008;105:19756–19761.
- [23] Yang J, Gao C, Chai L, Ma Y. A novel SALL4/OCT4 transcriptional feedback network for pluripotency of embryonic stem cells. *PLoS One* 2010;5:e10766.
- [24] Zhang J, Tam WL, Tong GQ, Wu Q, Chan HY, Soh BS, et al. Sall4 modulates embryonic stem cell pluripotency and early embryonic development by the transcriptional regulation of Pou5f1. *Nat Cell Biol* 2006;8:1114–1123.
- [25] Marquardt JU, Thorgeirsson SS. Sall4 in “stemness”-driven hepatocarcinogenesis. *New Engl J Med* 2013;368:2316–2318.
- [26] Oikawa T, Kamiya A, Zeniya M, Chikada H, Hyuck AD, Yamazaki Y, et al. SALL4, a stem cell biomarker in liver cancers. *Hepatology* 2013;57:1469–1483.
- [27] Lu J, Jeong HW, Kong N, Yang Y, Carroll J, Luo HR, et al. Stem cell factor SALL4 represses the transcriptions of PTEN and SALL1 through an epigenetic repressor complex. *PLoS One* 2009;4:e5577.
- [28] Lai AY, Wade PA. Cancer biology and NuRD: a multifaceted chromatin remodelling complex. *Nat Rev Cancer* 2011;11:588–596.
- [29] Chou DM, Adamson B, Dephoure NE, Tan X, Nottke AC, Hurov KE, et al. A chromatin localization screen reveals poly (ADP ribose)-regulated recruitment of the repressive polycomb and NuRD complexes to sites of DNA damage. *Proc Natl Acad Sci USA* 2010;107:18475–18480.
- [30] Larsen DH, Poinssignon C, Gudjonsson T, Dinant C, Payne MR, Hari FJ, et al. The chromatin-remodeling factor CHD4 coordinates signaling and repair after DNA damage. *J Cell Biol* 2010;190:731–740.
- [31] Pan MR, Hsieh HJ, Dai H, Hung WC, Li K, Peng G, et al. Chromodomain helicase DNA-binding protein 4 (CHD4) regulates homologous recombination DNA repair, and its deficiency sensitizes cells to poly(ADP-ribose) polymerase (PARP) inhibitor treatment. *J Biol Chem* 2012;287:6764–6772.
- [32] Polo SE, Kaidi A, Baskcomb L, Galanty Y, Jackson SP. Regulation of DNA-damage responses and cell-cycle progression by the chromatin remodelling factor CHD4. *EMBO J* 2010;29:3130–3139.
- [33] Yamashita T, Honda M, Takatori H, Nishino R, Minato H, Takamura H, et al. Activation of lipogenic pathway correlates with cell proliferation and poor prognosis in hepatocellular carcinoma. *J Hepatol* 2009;50:100–110.
- [34] Yamashita T, Honda M, Nio K, Nakamoto Y, Takamura H, Tani T, et al. Oncostatin m renders epithelial cell adhesion molecule-positive liver cancer stem cells sensitive to 5-Fluorouracil by inducing hepatocytic differentiation. *Cancer Res* 2010;70:4687–4697.
- [35] Roessler S, Long EL, Budhu A, Chen Y, Zhao X, Ji J, et al. Integrative genomic identification of genes on 8p associated with hepatocellular carcinoma progression and patient survival. *Gastroenterology* 2012;142:e912.
- [36] Lee YH, Seo D, Choi KJ, Andersen JB, Won MA, Kitade M, et al. Antitumor effects in hepatocarcinoma of isoform-selective inhibition of HDAC2. *Cancer Res* 2014;74:4752–4761.
- [37] Raggi C, Factor VM, Seo D, Holczbauer A, Gillen MC, Marquardt JU, et al. Epigenetic reprogramming modulates malignant properties of human liver cancer. *Hepatology* 2014;59:2251–2262.
- [38] Smeenk G, Wiegant WW, Vrolijk H, Solari AP, Pastink A, van Attikum H. The NuRD chromatin-remodeling complex regulates signaling and repair of DNA damage. *J Cell Biol* 2010;190:741–749.
- [39] Zhang JX, Li DQ, He AR, Motwani M, Vasiliou V, Eswaran J, et al. Synergistic inhibition of hepatocellular carcinoma growth by cotargeting chromatin modifying enzymes and poly (ADP-ribose) polymerases. *Hepatology* 2012;55:1840–1851.